Trajectory Studies of S_N2 Nucleophilic Substitution. 5. Semiempirical Direct Dynamics of Cl^-- - -CH_3Br Unimolecular Decomposition

Gilles H. Peslherbe, Haobin Wang, and William L. Hase*

Contribution from the Department of Chemistry, Wayne State University, Detroit, Michigan 48202

Received September 11, 1995[⊗]

Abstract: Direct dynamics simulations of the dynamics of the Cl^-- - -CH_3Br complex are performed for 25 ps or until either $Cl^- + CH_3Br$ or $ClCH_3 + Br^-$ are formed. Two different potential energy surfaces, AM1-SRP1 and AM1-SRP2, are investigated in the simulations by using the AM1 semiempirical model with two different sets of specific reaction parameters (SRPs). The AM1-SRP surfaces give non-RRKM unimolecular dynamics for Cl^-- - -CH_3Br as found in a previous simulation based on an analytic potential energy surface, PES1(Br), derived by fitting HF/SV4PP/6-31G* *ab initio* calculations and experimental data. However, detailed aspects of the Cl^-- - -CH_3Br intramolecular and unimolecular dynamics are different for the two AM1-SRP surfaces and in some cases strikingly different from those found for the PES1(Br) surface. Global potential energy surface properties, not only those of stationary points and along the reaction path, are expected to influence the Cl^-- - -CH_3Br nonstatistical dynamics. Of the three surfaces, only PES1(Br) gives a relative translation energy distribution for the $ClCH_3 + Br^-$ dissociation products which agrees with experiment. The average product translational energy is approximately a factor of 3 too large for each of the AM1-SRP surfaces. A definitive determination of all the dynamics and kinetics for $Cl^- + CH_3Br \rightarrow ClCH_3 + Br^-$ S_N2 nucleophilic substitution may require dynamical calculations based on a potential energy surface derived from high-level *ab initio* calculations.

I. Introduction

In a recent series of papers[1−7] classical trajectory simulations have been used to study the elementary reaction dynamics of the gas-phase S_N2 nucleophilic substitution reactions $Cl_a^- + CH_3Cl_b \rightarrow Cl_aCH_3 + Cl_b^-$ and $Cl^- + CH_3Br \rightarrow ClCH_3 + Br^-$. The trajectories indicate that statistical theories may be of only limited use in interpreting the kinetics and dynamics of such S_N2 reactions.[8] The results of the trajectory simulations suggest the following: (1) The intramolecular vibrational modes of the CH_3Y reactant are weakly coupled to the relative motion of the $X^- + CH_3Y$ collision and X^-- - -CH_3Y complexes are formed by translation to rotation ($T \rightarrow R$) energy transfer.[5] Thus collisions, which do not have the proper dynamical stereochemistry and cannot transfer sufficient energy to rotation, do not form complexes. As a result,[3,5] the trajectory $X^- + CH_3Y \rightarrow X^-$- - -$CH_3Y$ association rate constant is smaller than that of statistical ion−molecule capture theories.[9] (2) Exciting the C−Y stretch mode of the reactant opens up a direct substitution mechanism, without trapping in either the X^-- - -CH_3Y or XCH_3- - -Y^- complex.[1,3,5] (3) Unimolecular decomposition rates of the ion−molecule complexes are mode specific because of weak coupling between the low-frequency intermolecular modes and the higher frequency intramolecular modes.[2,3,6,7] (4) $X^- + CH_3Y$ collisions form an intermolecular complex that is only weakly coupled to an intramolecular complex, for which energy has transferred from the low-frequency intermolecular modes to the higher frequency CH_3Y intramolecular modes. Because of this weak coupling, the intramolecular complex may remain trapped in the vicinity of the central barrier of the S_N2 reaction and multiple crossings of this barrier may occur before the trajectory forms products or returns to reactants.[4,6] (5) The $XCH_3 + Y^-$ products of the S_N2 reaction are formed with an energy distribution that does not agree[6] with the predictions of either phase space theory (PST)[10−12] or orbiting transition state/phase space theory (OTS/PST).[13]

Experimental studies support a number of the above trajectory simulation results. For highly exothermic S_N2 reactions, like $F^- + CH_3Cl$, CH_3Br, and CH_3I, the statistical theory S_N2 rate constant is predicted to equal the ion−molecule capture rate constant. In contrast, for such reactions the experimental rate constants of Su, DePuy, *et al.*[14,15] are smaller than the capture value, which is consistent with point (1) above. Experimental agreement with point (5) is found in the product energy partitioning studies of Graul and Bowers[16,17] for Cl^-- - -$CH_3Br \rightarrow ClCH_3 + Br^-$. Since the products are formed with less translational energy than predicted by either PST or OTS/PST, the implication is that the products are vibrationally hot. This implies, by microscopic reversibility,[16,17] that vibrational excita-

[⊗] Abstract published in *Advance ACS Abstracts,* February 1, 1996.

(1) Vande Linde, S. R.; Hase, W. L. *J. Am. Chem. Soc.* **1989**, *111*, 2349.
(2) Vande Linde, S. R.; Hase, W. L. *J. Phys. Chem.* **1990**, *94*, 6148.
(3) Vande Linde, S. R.; Hase, W. L. *J. Chem. Phys.* **1990**, *93*, 7962.
(4) Cho, Y. J.; Vande Linde, S. R.; Zhu, L.; Hase, W. L. *J. Chem. Phys.* **1992**, *96*, 8275.
(5) Hase, W. L.; Cho, Y. J. *J. Chem. Phys.* **1993**, *98*, 8626.
(6) Wang, H.; Peslherbe, G. H.; Hase, W. L. *J. Am. Chem. Soc.* **1994**, *116*, 9644.
(7) Peslherbe, G. H.; Wang, H.; Hase, W. L. *J. Chem. Phys.* **1995**, *102*, 5626.
(8) Hase, W. L. *Science* **1994**, *266*, 998.
(9) Hase, W. L.; Wardlaw, D. M. In *Bimolecular Collisions*; Ashfold, M. N. R., Baggot, J. E., Eds.; Royal Society of Chemistry: London, 1989; p 171.
(10) Light, J. C. *Discuss. Faraday Soc.* **1967**, *44*, 14.
(11) Klots, C. E. *J. Phys. Chem.* **1971**, *75*, 1526.
(12) Klots, C. E. *Z. Naturforsch., Teil A* **1972**, *27*, 553.
(13) Chesnavich, W. J.; Bowers, M. T. In *Gas Phase Ion Chemistry*; Bowers, M. T., Ed.; Academic Press: New York, 1979; Vol. 1, p 119.
(14) Su, T.; Morris, R. A.; Viggiano, A. A.; Paulson, J. F. *J. Phys. Chem.* **1990**, *94*, 8426.
(15) DePuy, C. H.; Gronert, S.; Mullin, A.; Bierbaum, V. M. *J. Am. Chem. Soc.* **1990**, *112*, 8650.
(16) Graul, S. T.; Bowers, M. T. *J. Am. Chem. Soc.* **1991**, *113*, 9696.
(17) Graul, S. T.; Bowers, M. T. *J. Am. Chem. Soc.* **1994**, *116*, 3875.

0002-7863/96/1518-2257$12.00/0

tion of the reactants promotes reaction, as discussed in point (2) above. There is no direct evidence from experimental studies for points (3) and (4) above, but indirect evidence comes from the inability of statistical theories to simultaneously fit the experimental data of Viggiano *et al.*[18,19] for $Cl^- + CH_3Br \rightarrow ClCH_3 + Br^-$ S_N2 nucleophilic substitution, which includes the rate constant versus temperature, the H/D kinetic isotope effect, and the rate constant versus relative translational energy and CH_3Br temperature.[20] Evidence for non-RRKM and non-TST behavior has been observed in other ion−molecule reactions,[21−28] like proton transfer.[27,28]

The aforementioned trajectory studies were performed with analytic potential energy functions[29,30] derived from fits to experimental and *ab initio* data. With the increased speed of computers, direct dynamics calculations[31−48] have become possible for performing such studies. Here, the trajectory is integrated "on the fly", without an analytic potential and its derivatives, by obtaining energy and derivatives directly from an electronic structure theory. Thus, there is no need for an intermediate analytical potential. For short-lived events, like motion off a potential energy barrier, *ab initio* trajectories (i.e. *ab initio* direct dynamics) are possible.[32,41−43] But, because of the time required to calculate the *ab initio* energies and derivatives, this approach cannot be used to follow long-time events like unimolecular decomposition from a potential energy well. However, for such problems, it is possible to perform semiempirical direct dynamics,[31,44−47] i.e. direct dynamics employing semiempirical molecular orbital (MO) electronic structure theories,[49,50] such as neglect of diatomic differential overlap (NDDO) methods.[51−56] Direct dynamics techniques have also been employed for calculating reaction rates by semiclassical methods.[57]

In the work presented here, semiempirical direct dynamics is used to simulate Cl^-- - -CH_3Br unimolecular decomposition, and compare with the results of the previous trajectory study,[6] which used an analytic potential derived in part from *ab initio* calculations.[30] These semiempirical direct dynamics are carried out by interfacing the general chemical dynamics computer program VENUS[58] with the semiempirical MO electronic structure theory computer package MOPAC 7.0.[59] The resulting program is called VENUS-MOPAC.[60] The AM1 parameters[54] in MOPAC, supplemented with two sets of specific reaction parametes (SRPs),[18,61−65] are used in these direct dynamics.

II. Properties of the Potential Energy Surfaces

The direct dynamics calculations reported here were performed using the AM1 semiempirical model[54] with two different sets of specific reaction parameters (SRPs).[18,61−65] The resulting two models are identified as AM1-SRP1 and AM1-SRP2. The parameters for AM1-SRP1 were chosen to give an approximate fit, using conventional transition state theory, to the $Cl^- + CH_3Br \rightarrow ClCH_3 + Br^-$ experimental rate constant versus temperature.[18] For AM1-SRP2 the parameters were chosen[66] to exactly reproduce the experimental kinetic isotope effect. In the following, properties of the AM1-SRP1 and AM1-SRP2 potential energy surfaces are compared with those of the AM1[54] and PM3[55−57] surfaces without SRPs, the HF/SV4PP/6-31G* and MP2/SV4PP/6-31G* surfaces,[30] and the analytic potential energy surface PES1(Br).[30] A comparison is also made with available experimental information.[16,67−72]

(18) Viggiano, A. A.; Paschkewitz, J. S.; Morris, R. A.; Paulson, J. F.; Gonzalez-Lafont, A.; Truhlar, D. G. *J. Am. Chem. Soc.* **1991**, *113*, 9404.
(19) Viggiano, A. A.; Morris, R. A.; Paschkewitz, J. S.; Paulson, J. F. *J. Am. Chem. Soc.* **1992**, *114*, 10477.
(20) Wang, H.; Hase, W. L. *J. Am. Chem. Soc.* **1995**, *117*, 9347.
(21) Swamy, K. N.; Hase, W. L. *J. Am. Chem. Soc.* **1984**, *106*, 4071.
(22) Hase, W. L.; Darling, C. L.; Zhu, L. *J. Chem. Phys.* **1992**, *96*, 8295.
(23) Wladkowski, B. D.; Wilbur, J. L.; Brauman, J. I. *J. Am. Chem. Soc.* **1992**, *114*, 9706.
(24) Wilbur, J. L.; Wladkowski, B. D.; Brauman, J. I. *J. Am. Chem. Soc.* **1993**, *115*, 10823.
(25) Ramachandran, R.; Ezra, G. S. *J. Chem. Phys.* **1992**, *97*, 6322.
(26) Ramachandran, R.; Ezra, G. S. *J. Phys. Chem.* **1995**, *99*, 2435.
(27) Lim, K. F.; Brauman, J. I. *J. Chem. Phys.* **1991**, *94*, 7164.
(28) Hinde, R. J.; Ezra, G. S. *Chem. Phys. Lett.* **1994**, *228*, 333.
(29) Vande Linde, S. R.; Hase, W. L. *J. Phys. Chem.* **1990**, *94*, 2778.
(30) Wang, H.; Zhu, L.; Hase, W. L. *J. Phys. Chem.* **1994**, *98*, 1608.
(31) Wang, I. S. Y.; Karplus, M. *J. Am. Chem. Soc.* **1973**, *95*, 8160.
(32) Leforestier, C. *J. Chem. Phys.* **1978**, *68*, 4406.
(33) Greer, J. C.; Ahlrichs, R.; Hertel, I. V. *Z. Phys. D* **1991**, *18*, 413.
(34) Maluendes, S. A.; Dupuis, M. *Int. J. Quantum Chem.* **1992**, *42*, 1327.
(35) Hartke, B.; Carter, E. A. *Chem. Phys. Lett.* **1992**, *189*, 358.
(36) Hartke, B.; Carter, E. A. *J. Chem. Phys.* **1992**, *97*, 6569.
(37) Hartke, B.; Gibson, D. A.; Carter, E. A. *Int. J. Quantum Chem.* **1993**, *45*, 59.
(38) Hartke, B.; Carter, E. A. *Chem. Phys. Lett.* **1993**, *216*, 324.
(39) Gibson, D. A.; Carter, E. A. *J. Phys. Chem.* **1993**, *97*, 13429.
(40) Jellinek, J.; Bonacic-Koutecky, V.; Fantucci, P.; Wiechert, M. *J. Chem. Phys.* **1994**, *101*, 10092.
(41) Helgaker, T.; Uggerud, E.; Jensen, H. J. A. *Chem. Phys. Lett.* **1990**, *173*, 145.
(42) Uggerud, E.; Helgaker, T. *J. Am. Chem. Soc.* **1992**, *114*, 4265.
(43) Chen, W.; Hase, W. L.; Schlegel, H. B. *Chem. Phys. Lett.* **1994**, *228*, 436.
(44) Field, M. J.; Bash, P. A.; Karplus, M. *J. Comput. Chem.* **1990**, *11*, 700.
(45) Zhao, X. G.; Carmer, C. S.; Weiner, B.; Frenklach, M. *J. Phys. Chem.* **1993**, *97*, 1639.
(46) Carmer, C. S.; Weiner, B.; Frenklach, M. *J. Chem. Phys.* **1993**, *99*, 1356.
(47) Long, X.; Graham, R. L.; Lee, C.; Smithline, S. *J. Chem. Phys.* **1994**, *100*, 7223.
(48) Peslherbe, G. H.; Hase, W. L. *J. Chem. Phys.* Submitted for publication.
(49) Stewart, J. P. In *Reviews in Computational Chemistry*; Lipkowitz, K. B., Boyd, D. B., Eds.; VCH Publishers Inc.: New York, 1990; Vol. 1, p 45.
(50) Zerner, M. C. In *Reviews in Computational Chemistry*; Lipkowitz, K. B., Boyd, D. B., Eds.; VCH Publishers Inc.: New York, 1991; Vol. 2, p 313.
(51) Pople, J. A.; Santry, D. P.; Segal, G. A. *J. Chem. Phys.* **1965**, *43*, S129.
(52) Dewar, M. J. S.; Thiel, W. *J. Am. Chem. Soc.* **1977**, *99*, 4899.
(53) Dewar, M. J. S.; Thiel, W. *J. Am. Chem. Soc.* **1977**, *99*, 4907.
(54) Dewar, M. J. S.; Zoebisch, E. G.; Healy, E. F.; Stewart, J. J. P. *J. Am. Chem. Soc.* **1985**, *107*, 3902.
(55) Stewart, J. J. P. *J. Comput. Chem.* **1989**, *10*, 209. Stewart, J. J. P. *J. Comput. Chem.* **1989**, *10*, 221.
(56) Stewart, J. J. P. *J. Comput. Chem.* **1991**, *12*, 320.
(57) Truhlar, D. G. In *The Reaction Path in Chemistry: Current Approaches and Perspectives*; Heidrich, D., Ed.; Kluwer: Dordrecht, 1995; p 229.
(58) Hase, W. L.; Duchovic, R. J.; Hu, X.; Lim, K.; Lu, D.-h.; Peslherbe, G. H.; Swamy, K. N.; Linde, S. R. V.; Wang, H.; Wolf, R. J. VENUS, a General Chemical Dynamics Computer Program. To be submitted to QCPE. VENUS is an enhanced version of MERCURY: Hase, W. L. *QCPE* **1983**, *3*, 453.
(59) Stewart, J. P. P. MOPAC 7.0, a General Molecular Orbital Package. *QCPE* **1993**, 455.
(60) Peslherbe, G. H.; Hase, W. L. VENUS-MOPAC, A General Chemical Dynamics and Semiempirical Direct Dynamics Computer Program. To be released.
(61) Gonzalez-Lafont, A.; Truong, T. N.; Truhlar, D. G. *J. Phys. Chem.* **1991**, *95*, 4618.
(62) Liu, Y.-P.; Lu, D.-h.; Gonzalez-Lafont, A.; Truhlar, D. G.; Garrett, B. C. *J. Am. Chem. Soc.* **1993**, *115*, 7806.
(63) Hu, W.-P.; Liu, Y.-P.; Truhlar, D. G. *J. Chem. Soc., Faraday Trans.* **1994**, *90*, 1715.
(64) Rossi, I.; Truhlar, D. G. *Chem. Phys. Lett.* **1994**, *233*, 231.
(65) Corchado, J. C.; Espinosa-Garcia, J.; Hu, W.-P.; Rossi, I.; Truhlar, D. G. *J. Phys. Chem.* **1995**, *99*, 687.
(66) Hu, W.-P.; Truhlar, D. G. Private communication.
(67) Graner, G. *J. Mol. Spectrosc.* **1981**, *90*, 394.
(68) Caldwell, G.; Magnera, T. F.; Kebarle, P. *J. Am. Chem. Soc.* **1984**, *106*, 959.
(69) Jensen, P.; Brodersen, S.; Guelachvili, G. *J. Mol. Spectrosc.* **1981**, *88*, 378.
(70) *CRC Handbook of Chemistry and Physics*, 73rd ed.; Weast, R. C., Ed.; CRC Press Inc.: Boca Raton, FL, 1992.

Table 1. Energies and Structures for Stationary Points[a]

property	exp.[b]	PES1(Br)[c]	*ab initio*[d]	AM1-SRP1[e]	AM1-SRP2[f]	AM1	PM3
			CH_3Br Reactant				
r_{C-Br}	1.934[g]	1.944	1.944(1.939)	1.895	1.892	1.905	1.951
r_{H-C}	1.082	1.077	1.077 (1.087)	1.109	1.109	1.110	1.090
θ_{H-C-Br}	107.7	107.6	107.8 (107.8)	108.4	108.8	108.8	108.4
energy	0	0	0	0	0	0	0
			Cl^-- - -CH_3Br Complex				
r_{C-Cl}		3.221	3.216	2.877	2.904	2.866	2.651
r_{C-Br}		1.991	1.997	1.929	1.934	1.948	2.036
r_{H-c}		1.071	1.071	1.109	1.085	1.108	1.087
θ_{H-C-Br}		107.1	106.8	109.3	108.6	108.3	105.1
energy	-10 ± 1[h]	−10.73	−10.74	−10.59	−9.13	−8.68	−12.16
			Central Barrier				
r_{C-Cl}		2.470	2.469	2.116	2.118	2.033	2.407
r_{C-Br}		2.462	2.458	2.275	2.250	2.359	2.168
r_{H-C}		1.062	1.062	1.096	1.075	1.098	1.082
θ_{H-C-Br}		92.6	92.2	89.4	90.1	85.7	98.5
energy		−2.78	−2.91	−1.52	−1.87	2.41	−11.61
			$ClCH_3$- - -Br^- Complex				
r_{C-Cl}		1.819	1.825	1.754	1.748	1.781	1.823
r_{C-Br}		3.527	3.517	3.197	3.273	3.095	2.787
r_{H-C}		1.074	1.073	1.110	1.089	1.110	1.092
θ_{H-C-Br}		71.9	72.2	70.8	70.9	72.4	72.0
energy	−16[h]	−21.21	−21.21	−13.62	−14.22	−2.98	−27.90
			CH_3Cl Product				
r_{C-Cl}	1.776[i]	1.789	1.789 (1.793)	1.732	1.723	1.741	1.764
r_{H-C}	1.085	1.077	1.076 (1.088)	1.110	1.091	1.112	1.094
θ_{H-C-Cl}	108.6	108.1	108.1 (108.1)	108.4	109.3	108.3	109.9
energy	−6,[j] −8,[k] −9[l]	−12.65	−12.63 (−11.34)	−6.29	−8.43	4.49	−17.72

[a] Energy is in kcal/mol, bond length in Å, and angle in deg. [b] The experimental relative energies are for 0 K. [c] Analytic potential energy surface from: Wang, H.; Zhu, L.; Hase, W. L. *J. Phys. Chem.* **1994**, *98*, 1608. [d] Hartree−Fock calculations with a SV4PP basis set for Cl and Br, and a 6-31G* basis set for CH_3. See: Wang, H.; Zhu, L.; Hase, W. L. *J. Phys. Chem.* **1994**, *98*, 1608. Geometries and energies for the MP2 level calculations with the same basis sets are given in parentheses. The listed relative energies are electronic energy differences without including zero-point energies. With zero-point energy included, the relative energy differences for the prereaction complex, the central barrier, the postreaction complex, and products are −10.32, −3.18, −20.06, and −11.85, respectively. Zero-point energy is calculated from the HF harmonic vibrational frequencies without scaling. [e] AM1 with specific reaction parameters (SRP) from: Viggiano, A. A.; Paschkewitz, J. S.; Morris, R. A.; Paulson, J. F.; Gonzalez-Lafont, A.; Truhlar, D. G. *J. Am. Chem. Soc.* **1991**, *113*, 9404. [f] AM1 with a second set of specific reaction parameters (SRP), which exactly reproduces the experimental kinetic isotope effect: Hu, W.-P.; Truhlar, D. G. Private communication. [g] The CH_3Br experimental geometry is taken from: Graner, G. *J. Mol. Spectrosc.* **1981**, *90*, 394. [h] Caldwell, G.; Magnera, T. K.; Kebarle, P. *J. Chem. Soc.* **1984**, *106*, 959. [i] The CH_3Cl experimental geometry is taken from: Jensen, P.; Brodersen, S.; Guelachvili, G. *J. Mol. Spectrosc.* **1987**, *88*, 378. [j] Viggiano, A. A.; Paschkewitz, J. S.; Morris, R. A.; Paulson, J. F.; Gonzalez-Lafont, A.; Truhlar, D. G. *J. Am. Chem. Soc.* **1991**, *113*, 9404. Graul, S. T.; Bowers, M. T. *J. Am. Chem. Soc.* **1991**, *113*, 9696. [k] Caldwell, G.; Magnera, T. F.; Kebarle, P. *J. Am. Chem. Soc.* **1984**, *106*, 959. *CRC Handbook of Chemistry and Physics*, 73rd ed.; Weast, R. C., Ed.; CRC Press Inc.: Boca Raton, FL, 1992. Lias, S. G.; Bartmess, J. E.; Liebman, J. F.; Holmes, J. L.; Levin, R. D.; Mallard, W. G. *J. Phys. Chem. Ref. Data* **1988**, *17*, *Suppl. 1*, 1. [l] The reported C−Cl and C−Br bond energies and Cl and Br electron affinities, [*CRC Handbook of Chemistry and Physics*, 73rd ed.; Weast, R. C., Ed.; CRC Press Inc.: Boca Raton, FL, 1992. Lias, S. G.; Bartness, J. E.; Liebman, J. F.; Holmes, J. L.; Levin, R. D.; Mallard, W. G. *J. Phys. Chem. Ref. Dat* **1988**, *17*, *Suppl. 1*, 1] gives a 0 K heat of reaction of −9 kcal/mol.

Energies and geometries for the stationary points of the different $Cl^- + CH_3Br \rightarrow ClCH_3 + Br^-$ potential energy surfaces are compared in Table 1. The HF and MP2 *ab initio* surfaces give CH_3Br and CH_3Cl geometries and a Cl^-- - -CH_3-Br well depth in good agreement with experiment. The analytic potential energy surface PES1(Br) was chosen to fit the structures and energies of the HF stationary points. A major difference between the AM1-SRP surfaces and the *ab initio* surfaces is that the C−Cl and C−Br bond lengths are larger for the latter, particularly for the complexes and central barrier. The *ab initio* surfaces give energies for the $ClCH_3$- - -Br^- complex and $ClCH_3 + Br^-$ products which are lower than the experimental values, while the AM1-SRP surfaces are parametrized to fit these energies. At the central barrier the analytic potential PES1(Br) mimics the *ab initio* HF/SV4PP/6-31G* calculations and gives a C−Cl bond length r_{Cl-C} only slightly larger than r_{Br-C}. In contrast, r_{Br-C} is 0.15 Å longer than r_{Cl-C} for the AM1-SRP surfaces. This appears to arise from the AM1 model which gives r_{Br-C} 0.3 Å longer than r_{Cl-C}. The PM3 model reverses the relationship between the bond lengths and gives r_{Cl-C} 0.24 Å longer. The minimum energy path potential energy profiles are shown in Figure 1 for the different surfaces considered here.

High-level *ab initio* calculations have been performed for the $Cl^- + CH_3Cl$ reactive system[73−75] and they give a C−Cl bond length at the central barrier similar to the 2.383 Å found from a HF/6-31G* calculation.[29,76] Calculations performed at the MP2/6-31+G(d) level of theory[74] give a value of 2.317 Å for this bond length and an unpublished CEPA-1 calculation[75] with a 6-311+G(2df,p) type basis set gives 2.323 Å. For the $Cl^- + CH_3Br$ system, a MP2/6-31+G(d) calculation[77] gives central barrier C−Cl and C−Br bond lengths of 2.371 and 2.430 Å, respectively. A MP2/PTZ+ calculation[78] gives a value of 2.322

(71) Lias, S. G.; Bartmess, J. E.; Liebman, J. F.; Holmes, J. L.; Levin, R. D.; Mallard, W. G. *J. Phys. Chem. Ref. Data* **1988**, *17*, *Suppl. 1*, 1.
(72) Duncan, J. L.; Allan, A.; McKean, D. C. *Mol. Phys.* **1970**, *18*, 289.
(73) (a) Tucker, S. C.; Truhlar, D. G. *J. Phys. Chem.* **1989**, *93*, 8138. (b) Vetter, R.; Zülicke, L. *J. Am. Chem. Soc.* **1990**, *112*, 5136.
(74) Glukhovtsev, M. N.; Pross, A.; Radom, L. *J. Am. Chem. Soc.* **1995**, *117*, 2024.
(75) Seeger, S.; Botschwina, P. Private communication.
(76) Huston, S. E.; Rossky, P. J.; Zichi, D. A. *J. Chem. Phys.* **1989**, *111*, 5680.
(77) Glukhovtsev, M. N.; Pross, A.; Radom, L. *J. Am. Chem. Soc.* Submitted for publication.

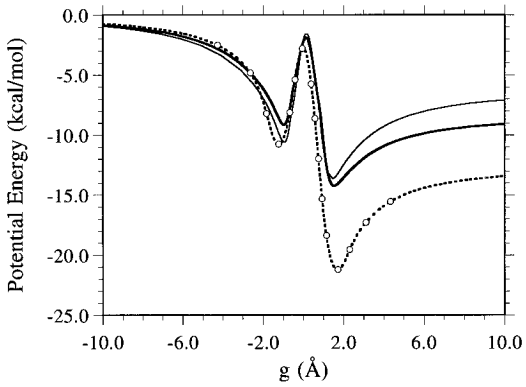

Figure 1. $Cl^- + CH_3Br \rightarrow ClCH_3 + Br^-$ minimum energy path energy profile as a function of $g = r_{C-Br} - r_{C-Cl}$ for the different potential energy surfaces considered here: *ab initio* HF/SV4PP/6-31G* (○); PES1(Br) analytic function (- - -); AM1-SRP1 (—) and AM1-SRP2 (bold solid curve) models.

Å for the C−Cl bond length and 2.392 Å for the C−Br bond length. Both of these calculations indicate the C−Cl bond length is slightly shorter than the C−Br bond length at the central barrier. The HF/SV4PP/6-31G* calculation gives similar values for these bond lengths at the central barrier.

The harmonic vibrational frequencies for CH_3Br and CH_3Cl, determined from experiment and from the potential energy surfaces, are compared in Table 2. The only striking disparity between the sets of frequencies is that the ordering of the A_1, C−H stretch and E, C−H stretch is reversed between the *ab initio* and analytic potentials and the semiempirical potentials. Frequencies determined for the central barrier and the Cl^-- - -CH_3Br and $ClCH_3$- - -Br^- complexes, from the different potential energy surfaces and from scaling the *ab initio* frequencies, are compared in Table 3. The scale factor used in the scaling was determined by comparing experimental and *ab initio* frequencies for CH_3Br and CH_3Cl.[30] The major difference between these frequencies for the AM1-SRP and the PES1(Br) and PES2(Br) analytic surfaces is that the former surfaces give higher C−Cl and C−Br stretching frequencies. This result seems consistent with the shorter C−Cl and C−Br bond lengths for the complexes and central barrier on the AM1-SRP surfaces (see Table 1).

The SRP parameters were chosen to improve the relative AM1 energies for the stationary points.[18,66] However, this clearly does not ensure accurate energies for other regions of the potential energy surface. An example of this is illustrated in Figure 2, where potential energy curves are plotted versus the C−Br bond length for stretching both the C−Br and C−Cl bonds and maintaining the difference in their bond lengths at the central barrier value $g^{\ddagger}$. The PES1(Br) surface gives 72.3 kcal/mol for the potential curve's asymptotic limit, which was chosen to approximate the experimental C−Br bond dissociation energy $\Delta H^{\circ}_{298} = 70.0 \pm 1.2$ kcal/mol. In contrast, the RHF AM1(SRP) models dissociate to a much higher asymptotic limit.

III. Details of the Direct Dynamics Simulations

The semiempirical direct dynamics simulations reported here were performed by interfacing the general chemical dynamics computer program VENUS[58] with the semiempirical MO electronic structure theory computer package MOPAC 7.0.[59] The trajectories were started from the prereaction complex Cl^-- - -CH_3Br to model experiments by Graul and Bowers,[16,17] and Cyr *et al.*,[79] and to compare with the previous simulations on the PES1(Br) analytic potential energy surface.[6]

A. Initial Conditions. Different initial non-random energy distributions for the Cl^-- - -CH_3Br prereaction complex on the AM1-SRP1 and AM1-SRP2 potential energy surfaces were investigated. The total energy of this complex, in excess of the $Cl^- + CH_3Br$ reactants classical asymptotic limit, is the harmonic zero-point energy of the Cl^-- - -CH_3Br complex plus approximately 2.7 kcal/mol. Since the zero-point energy of this complex differs from that of $Cl^- + CH_3Br$ by at most several tenths of a kcal/mol, the 2.7 kcal/mol approximately represents the excess energy of a $Cl^- + CH_3Br$ collision forming Cl^-- - -CH_3Br. An average thermal rotational energy at 300 K was included in the initial energy of Cl^-- - -CH_3Br by adding $RT/2$ to each principal axis of rotation. This corresponds to a total angular momentum of $84\hbar$, which, because of the shorter Cl^-- - -C and C−Br bonds on the AM1-SRP surfaces, is smaller than the corresponding value of $91\hbar$ on the PES1(Br) surface.[6]

For each of the initial conditions, zero-point energy is added and an individual normal mode of Cl^-- - -CH_3Br is excited, so that the total energy in excess of the $Cl^- + CH_3Br$ harmonic zero-point level is approximately 2.7 kcal/mol. The normal mode model is sufficiently accurate for adding zero-point energy to the Cl^-- - -CH_3Br complex and exciting a CH_3Br intramolecular mode of the complex.[4] In this model, the energy for a normal mode is distributed randomly between potential and kinetic by choosing a random phase for the normal mode. However, the three intermolecular modes of the Cl^-- - -CH_3Br complex (i.e. one stretching and two bendings) are very anharmonic with low frequencies and this normal mode model is not sufficiently accurate for exciting an intermolecular mode for the AM1-SRP1 and AM1-SRP2 models. To overcome this problem, only kinetic energy was added when exciting an intermolecular normal mode by adding either positive or negative momentum to the mode. In this manner, the problem with anharmonicity was avoided and the normal mode model was maintained for studying selective excitation of the intermolecular modes. Finally, when exciting two degenerate E modes, like the Cl^-- - -C bending, equal amounts of quanta are added to each of the degenerate modes.

The algorithms used to select the above initial conditions for the Cl^-- - -CH_3Br complex are standard options in VENUS and have been described in considerable detail elsewhere.[80]

B. Integrating the Classical Equations of Motion. The atomic motion is evaluated in the traditional classical trajectory fashion, as implemented in VENUS, by solving Hamilton's equations[81] with a combined fourth-order Runge−Kutta and sixth-order Adams−Moulton predictor−corrector numerical integration algorithm.[82] At each step of the integration, the Schrödinger equation is solved for electronic energies and forces on the nuclei within the framework of restricted Hartree−Fock (RHF) self-consistent-field (SCF) theory, under the NDDO approximation, by calling the appropriate routines of MOPAC 7.0. Once a converged SCF has been obtained, the first derivatives of the energy with respect to the Cartesian positions are evaluated analytically within MOPAC 7.0. The criterion for obtaining a converged self-consistent field is that the energy of two successive SCF iterations differs by less than 10^{-10} kcal/mol, so that with such a stringent criterion, the SCF energy is continuous to at least numerical precision. The starting point of the SCF calculation is taken to be the set of molecular orbital coefficients from the previous trajectory step, and, thus, if the geometry is changing smoothly in time, very few SCF iterations are needed at each point.

Integration of the equations of motion is performed with a step size of 0.1 fs, which ensures energy conservation to 5 places along a trajectory. A few trajectories were integrated with a step size 10 times as small, with initial conditions of various excitation types, but no major difference was observed in the dynamics and the energy conservation was not improved. Trajectories are propagated until dissociation occurs or up to 25 ps. It should be pointed out that the energy conservation obtained on such a significantly long time scale is rather good, and of the same order of magnitude as for previous trajectory calculations performed on analytic potential energy surfaces.[6] The actual CPU time required to integrate a trajectory up to 25 ps with a step size of 0.1 fs

(78) Hu, W.-P.; Truhlar, D. G. *J. Am. Chem. Soc.* **1995**, *117*, 10726.
(79) Cyr, D. M.; Posey, L. A.; Bishea, G. A.; Han, C.-C.; Johnson, M. A. *J. Am. Chem. Soc.* **1991**, *113*, 9697.
(80) Sloane, C. S.; Hase, W. L. *J. Chem. Phys.* **1977**, *66*, 1523.
(81) Goldstein, H. *Classical Mechanics*, 2nd ed.; Addison-Wesley: Reading, 1980.
(82) Bunker, D. L. *Methods Comput. Phys.* **1971**, *10*, 287.

Table 2. CH_3Br and CH_3Cl Harmonic Vibrational Frequencies[a]

mode	*ab initio*[b]	exp.[c]	PES1(Br)[d]	PES2(Br)[d]	AM1-SRP1[e]	AM1-SRP2[f]	AM1	PM3
				CH_3Br				
C−Br str. (A_1)	642	617	620	617	666	670	666	658
CH_3 rock (E)	1066	974	1065	927	882	889	889	979
CH_3 deform. (A_1)	1484	1333	1497	1374	1305	1330	1317	1336
CH_3 deform. (E)	1620	1472	1457	1442	1340	1354	1372	1369
C−H str. (A_1)	3278	3082	3048	3047	3187	3165	3163	3208
C−H str. (E)	3392	3184	3183	3182	3095	3048	3083	3160
				CH_3Cl				
C−Cl str. (A_1)	774	710	739	735	853	863	835	677
CH_3 rock (E)	1130	1038	1108	968	973	990	985	1008
CH_3 deform. (A_1)	1528	1383	1550	1423	1337	1358	1346	1345
CH_3 deform. (E)	1627	1482	1460	1440	1342	1365	1368	1384
C−H str. (A_1)	3268	3074	3050	3050	3179	3456	3151	3194
C−H str. (E)	3374	3166	3181	3181	3090	3037	3076	3123

[a] Frequency unit is cm^{-1}. [b] Frequencies calculated at the HF/SV4PP/6-31G* level of theory. See: Wang, H.; Zhu, L.; Hase, W. L. *J. Phys. Chem.* **1994**, *98*, 1608. [c] Duncan, J. L.; Allan, A.; McKean, D. C. *Mol. Phys.* **1970**, *18*, 289. [d] For PES1(Br) the H−C−Cl and H−C−Br bending force constants are the *ab initio* values, while these *ab initio* force constants are scaled for PES2(Br) to obtain better agreement with experiment. See: Wang, H.; Zhu, L.; Hase, W. L. *J. Phys. Chem.* **1994**, *98*, 1608. [e] AM1 with specific reaction parameters (SRP) from: Viggiano, A. A.; Paschkewitz, J. S.; Morris, R. A.; Paulson, J. F.; Gonzalez-Lafont, A.; Truhlar, D. G. *J. Am. Chem. Soc.* **1991**, *113*, 9404. [f] AM1 with a second set of specific reaction parameters (SRP), which exactly reproduces the experimental kinetic isotope effect: Hu, W.-P.; Truhlar, D. G. Private communication.

Table 3. Harmonic Vibrational Frequencies for the Complexes and Central Barrier[a]

mode	*ab initio*[b]	scaled[c]	PES1(Br)[d]	PES2(Br)[d]	AM1-SRP1[e]	AM1-SRP2[f]	AM1	PM3
				Cl^-- - -CH_3Br Complex				
Cl^- bend (E)	71	64	72	72	64	86	75	127
C−Cl str. (A_1)	94	90	91	91	120	111	117	141
C−Br str. (A_1)	518	498	500	499	590	591	591	446
CH_3 rock (E)	1032	943	1089	956	840	880	854	980
CH_3 deform. (A_1)	1420	1276	1467	1344	1242	1274	1266	1262
CH_3 deform. (E)	1595	1450	1452	1434	1331	1342	1363	1326
C−H str. (A_1)	3334	3134	3147	3147	3195	3178	3172	3180
C−H str. (E)	3471	3258	3293	3293	3092	3062	3094	3182
				Central Barrier				
Cl−C−Br bend (E)	183	165	169	146	204	212	198	184
Cl−C−Br str. (A_1)	172	164	161	161	224	226	219	217
CH_3 rock (E)	974	895	1155	995	942	1024	974	1053
out-of-plane bend (A_2)	1203	1089	1185	1023	1079	1173	1092	1230
CH_3 deform. (E)	1549	1411	1340	1339	1298	1311	1323	1277
C−H str. (A_1)	3418	3215	3215	3215	3198	3179	3167	3131
C−H str. (E)	3630	3406	3415	3415	3192	3145	3170	3204
reaction coordinate	380i		400i	400i	460i	403i	404i	339i
				$ClCH_3$- - -Br^- Complex				
Br^- bend (E)	65	58	64	64	41	57	68	167
C−Br str. (A_1)	70	67	68	68	84	73	91	194
C−Cl str. (A_1)	674	644	646	644	779	790	720	573
CH_3 rock (E)	1099	1010	1123	987	931	967	938	1062
CH_3 deform. (A_1)	1483	1342	1548	1418	1300	1334	1298	1353
CH_3 deform. (E)	1610	1467	1462	1439	1336	1349	1361	1368
C−H str. (A_1)	3314	3117	3101	3101	3188	3168	3160	3182
C−H str. (E)	3438	3226	3238	3238	3087	3048	3090	3142

[a] Frequency unit is cm^{-1}. [b] The *ab initio* calculations were performed at the HF/SV4PP/6-31G* level of theory, see: Wang, H.; Zhu, L.; Hase, W. L. *J. Phys. Chem.* **1994**, *98*, 1608. [c] Scale factors determined from the CH_3Br and CH_3Cl *ab initio* and experimental frequencies were used to scale *ab initio frequencies* for the complexes and central barrier, see: Wang, H.; Zhu, L.; Hase, W. L. *J. Phys. Chem.* **1994**, *98*, 1608. [d] For PES1(Br) the H−C−Cl and H−C−Br bending force constants are the *ab initio* values, while these *ab initio* force constants are scaled for PES2(Br) to obtain better agreement with experiment, see: Wang, H.; Zhu, L.; Hase, W. L. *J. Phys. Chem.* **1994**, *98*, 1608. [e] AM1 with specific reaction parameters (SRP) from: Viggiano, A. A.; Paschkewitz, J. S.; Morris, R. A.; Paulson, J. F.; Gonzalez-Lafont, A.; Truhlaer, D. G. *J. Am. Chem. Soc.* **1991**, *113*, 9404. [f] AM1 with a second set of specific reaction parameters (SRP), which exactly reproduces the experimental kinetic isotope effect: Hu, W.-P.; Truhlar, D. G. Private Communication. Hu, W.-P.; Truhlar, D. G. *J. Am. Chem. Soc.* **1995**, *117*, 10726.

is about 12 h on an IBM RS/6000 370 workstation, whose theoretical peak performance is about 26 MFlops. Integrating 400 trajectories (50 for each of the initial condition excitation types) with the AM1-SRP model thus would take about 6 months of CPU on the aforementioned workstation. Fortunately, most of the trajectories dissociate before the 25-ps limit and the actual computational cost of the trajectories is decreased by half.

C. Analysis of the Trajectory Results. The trajectories were analyzed for lifetimes of the Cl^-- - -CH_3Br and $ClCH_3$- - -Br^- complexes, and [Cl- - -CH_3- - -Br]$^-$ central barrier crossings. Each trajectory was initialized in the Cl^-- - -CH_3Br well and the time (i.e. lifetime) the trajectory remained in this well was recorded. If the trajectory dissociated to $Cl^- + CH_3Br$ reactants, the lifetime was taken as the last inner turning point in the $Cl^- + CH_3Br$ relative motion before dissociation. For isomerization to $ClCH_3$- - -Br^-, the lifetime was taken as the time the trajectory passed the central barrier, where $g = r_{C-Br} - r_{C-Cl}$ is given by 0.159 and 0.132 Å for AM1-SRP1 and AM1-SRP2, respectively. Once the central barrier was crossed the trajectory was analyzed to determine whether it proceeded directly to $ClCH_3 + Br^-$ products, without an inner turning point in the $ClCH_3 + Br^-$ relative motion. If not, the lifetime of the resulting $ClCH_3$- - -Br^- complex was recorded as described above for the Cl^-- - -CH_3Br complex.

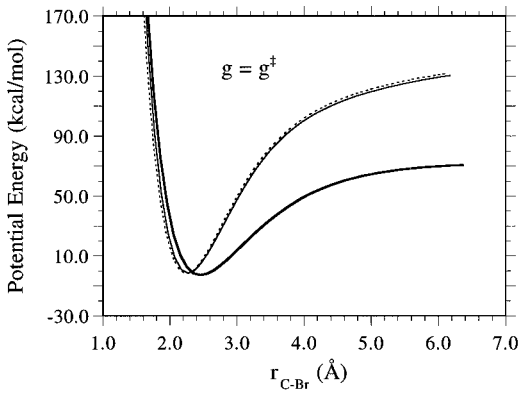

Figure 2. Potential energy curves, for the $[Cl\text{- - -}CH_3\text{- - -}Br]^-$ configuration, determined by stretching the C−Cl and C−Br bonds and holding $g = r_{C-Br} - r_{C-Cl}$ at the central barrier value $g^{\ddagger}$: AM1-SRP1 (—); AM1-SRP2 (- - -); and PES1(Br) (bold solid curve).

IV. RRKM Rate Constants

To assist in interpreting the trajectory calculations reported here, it is useful to have RRKM rate constants for the various unimolecular steps possibly participating in the $Cl^- + CH_3Br \rightarrow ClCH_3 + Br^-$ S_N2 reaction. A vibrator transition state model[9,83,84] was used for the RRKM calculations. The rotational degree of freedom associated with the K quantum number is assumed to be active so that the RRKM rate constant is written as[85−88]

$$k(E,J) = \frac{\sum_{K=-J}^{J} N^{\ddagger}[E - E_0 - E_r^{\ddagger}(J,K)]}{h \sum_{K=-J}^{J} \rho[E - E_r(J,K)]}$$

where $N^{\ddagger}$ is the transition state sum of states, ρ is the reactant density of states, E_0 is the transition state potential energy, and E_r is the symmetric top rotational energy. Treating K as active is based on the assumption that there is extensive vibrational/rotational coupling in the ion−dipole complexes.[88] Such coupling seems likely in the loose and floppy complexes.[8] If there is not extensive vibrational/rotational coupling, K may be treated as an adiabatic degree of freedom.[88] RRKM calculations may be performed for modes in which K is treated differently in the reactant and transition state, e.g. active for the reactant, but adiabatic for the transition state.[88] Specific vibrational degrees of freedom may also be treated as adiabatic in RRKM calculations.[7]

The variational version of RRKM theory[89] is used to calculate the transition state properties for $Cl^-\text{- - -}CH_3Br \rightarrow Cl^- + CH_3Br$ and $ClCH_3\text{- - -}Br^- \rightarrow ClCH_3 + Br^-$ dissociation. The path of steepest descent in mass-weighted Cartesian coordinates[90] and the reaction path Hamiltonian[91−93] were used to find properties along the reaction paths for these dissociations. The variational transition state for $Cl^-\text{- - -}CH_3Br \leftrightarrow ClCH_3\text{- - -}Br^-$ isomerization is located at the saddlepoint for the central barrier.

Table 4. Harmonic RRKM Rate Constants for the $Cl^-\text{- - -}CH_3Br$ and $ClCH_3\text{- - -}Br^-$ Complexes on Different Potential Energy Surfaces[a]

	rate constants[b]	
surface	quantum	classical
$Cl^-\text{- - -}CH_3Br \rightarrow Cl^- + CH_3Br$		
PES1(Br)	0.35	1.3
AM1-SRP1	0.33	2.2
AM1-SRP2	0.54	2.5
$Cl^-\text{- - -}CH_3Br \rightarrow ClCH_3\text{- - -}Br^-$		
PES1(Br)	0.03[c]	0.12
AM1-SRP1	0.003	0.03
AM1-SRP2	0.01	0.07
$ClCH_3\text{- - -}Br^- \rightarrow Cl^-\text{- - -}CH_3Br$		
PES1(Br)	0.0007	0.006
AM1-SRP1	0.0005	0.005
AM1-SRP2	0.0007	0.007
$ClCH_3\text{- - -}Br^- \rightarrow ClCH_3 + Br^-$		
PES1(Br)	1.6	1.6
AM1-SRP1	1.0	2.3
AM1-SRP2	1.8	2.7

[a] The total energy, in excess of the $Cl^- + CH_3Br$ classical asymptotic limit, is the $Cl^-\text{- - -}CH_3Br$ harmonic zero-point energy plus 2.7 kcal/mol. Inluded in this energy is $RT/2$ about each axis of $Cl^-\text{- - -}CH_3Br$, where $T = 300$ K. The resulting total angular momentum is 91 and 84 $\hbar$ for the PES1(Br) and AM1-SRP surfaces, respectively. [b] Rate constants are in units of ps^{-1}. [c] In ref 6, this rate constant was previously incorrectly reported as 0.006 ps^{-1}.

The above vibrator/reaction path variational RRKM model is expected to accurately represent $Cl^-\text{- - -}CH_3Br$ and $ClCH_3\text{- - -}Br^-$ dissociation. A flexible transition state model[94−98] has also been used in variational RRKM calculations. For $Cl^-\text{- - -}CH_3Cl \rightarrow Cl^- + CH_3Cl$ dissociation at 300 K, a calculation of this type, which implicitly includes a consideration of the variation of the reaction coordinate away from the center-of-mass separation distance, gives the same rate constant as determined with the type of vibrator/reaction path variational RRKM calculations performed here.[99] In addition, for $Cl^- + CH_3Br \rightarrow Cl^-\text{- - -}CH_3Br$ association in the 100−1000 K temperature range, the vibrator/reaction path variational transition state model gives rate constants nearly the same[30] as those determined with the statistical adiabatic channel model (SACM),[100] the orbiting transition state microcanonical variational transition state model,[13,101] and the trajectory capture model.[102]

Listed in Table 4 are both quantum and classical RRKM rate constants for dissociation and isomerization of the $Cl^-\text{- - -}CH_3Br$ and $ClCH_3\text{- - -}Br^-$ complexes. The rate constants are evaluated at the same total energy at which the trajectories were calculated. The classical RRKM rate constants are larger than the quantum values, since all the zero-point energy of the complex is free to assist dissociation in the classical calculation.[103] The difference, between the classical and quantum

(83) Aubanel, E. E.; Wardlaw, D. M.; Zhu, L.; Hase, W. L. *Int. Rev. Phys. Chem.* **1991**, *10*, 249.
(84) Zhu, L.; Hase, W. L. RRKM, a General RRKM Computer Program. *QCPE* **1995**, *14*, 644.
(85) Quack, M.; Troe, J. *Ber. Bunsenges. Phys. Chem.* **1974**, *78*, 240.
(86) Miller, W. H. *J. Am. Chem. Soc.* **1979**, *101*, 6810.
(87) Zhu, L.; Hase, W. L. *Chem. Phys. Lett.* **1990**, *175*, 117.
(88) Zhu, L.; Chen, W.; Hase, W. L.; Kaiser, E. W. *J. Phys. Chem.* **1993**, *97*, 311.
(89) Hase, W. L. *Acc. Chem. Res.* **1983**, *16*, 258.
(90) Truhlar, D. G.; Kuppermann, A. *J. Am. Chem. Soc.* **1970**, *93*, 1840. Fukui, K. In *The World of Quantum Chemistry*; Daudel, R., Pullman, B., Eds.; Reidel: Dordrecht, 1974; p 113.
(91) Miller, W. H.; Handy, N. C.; Adams, J. E. *J. Chem. Phys.* **1980**, *72*, 99.
(92) Kato, S.; Morokuma, K. *J. Chem. Phys.* **1980**, *73*, 3900.
(93) Morokuma, K.; Kato, S. In *Potential Energy Surfaces and Dynamics Calculations*; Truhlar, D. G., Ed.; Plenum: New York, 1981; p 243.
(94) Wardlaw, D. M.; Marcus, R. A. *J. Phys. Chem.* **1986**, *90*, 5383.
(95) Wardlaw, D. M.; Marcus, R. A. *Adv. Chem. Phys.* **1988**, *70*, 231.
(96) Aubanel, E. E.; Wardlaw, D. M. *J. Phys. Chem.* **1989**, *93*, 3117.
(97) Klippenstein, S. J. *J. Chem. Phys.* **1991**, *94*, 6469.
(98) Klippenstein, S. J. *J. Chem. Phys.* **1992**, *96*, 367.
(99) Klippenstein, S. J. Private communication.
(100) Troe, J. *Chem. Phys. Lett.* **1985**, *122*, 425.
(101) Chesnavich, W. J.; Su, T.; Bowers, M. T. *J. Chem. Phys.* **1980**, *72*, 2641.
(102) Su, T.; Chesnavich, W. J. *J. Chem. Phys.* **1982**, *76*, 5183.

Table 5. Number of Different Events for Quasiclassical Trajectories on the Different Potential Energy Surfaces[a]

excitation type	vibrational energy[b]	form reactants[c]	form products[d]	remain in complex A[e]	remain in complex B[f]	A → B crossings
			PES1(Br)			
1 Cl^- bend (E)	12.35 (60)	88 (0)[g]	2 (0)[g]	6 (1)[g]	4 (1)[g]	8
2 C−Cl str. (A_1)	12.48 (48)	100 (0)	0 (0)	0 (0)	0 (0)	0
3 C−H str. (E)	12.52 (1.3)	4 (3)	17 (4)	15 (6)	64 (31)	159
4 C−H str. (A_1)	12.60 (1.4)	2 (1)	17 (13)	8 (3)	73 (29)	183
5 CH_3 rock (E)	12.45 (4)	3 (3)	26 (12)	13 (4)	58 (26)	169
6 CH_3 deform. (E)	12.45(3)	1 (1)	23 (16)	10 (5)	66 (33)	191
7 CH_3 deform. (A_1)	12.58 (3)	5 (4)	25 (16)	13 (6)	57 (25)	164
8 C−Br str. (A_1)	12.86 (9)	1 (1)	28 (23)	8 (8)	63 (44)	236
			AM1-SRP1			
1 Cl^- bend (E)	12.44 (68)	88 (0)[g]	2 (0)[g]	10 (0)[g]	0 (0)[g]	2
2 C−Cl str. (A_1)	12.35 (36)	96 (0)	4 (0)	0 (0)	0 (0)	4
3 C−H str. (E)	12.37 (1.4)	76 (0)	2 (0)	20 (0)	2 (0)	4
4 C−H str. (A_1)	12.42 (1.4)	76 (0)	2 (0)	22 (0)	0 (0)	2
5 CH_3 rock (E)	12.01 (5)	62 (0)	14 (0)	18 (2)	6 (0)	22
6 CH_3 deform. (E)	12.18 (3.2)	76 (0)	4 (9)	20 (2)	0 (0)	8
7 CH_3 deform. (A_1)	12.43 (3.5)	68 (0)	6 (2)	24 (0)	2 (0)	10
8 C−Br str. (A_1)	12.65 (7.5)	48 (6)	32 (2)	16 (0)	4 (0)	44
			AM1-SRP2			
1 Cl^- bend (E)	10.76 (44)	80 (0)[g]	6 (0)[g]	10 (0)[g]	4 (0)[g]	5
2 C−Cl str. (A_1)	10.75 (34)	100 (0)	0 (0)	0 (0)	0 (0)	0
3 C−H str. (E)	10.50 (1.2)	64 (0)	8 (0)	26 (0)	2 (0)	10
4 C−H str. (A_1)	10.90 (1.2)	54 (0)	12 (0)	34 (0)	0 (0)	12
5 CH_3 rock (E)	11.07 (4.4)	48 (0)	6 (0)	46 (0)	0 (0)	6
6 CH_3 deform. (E)	10.74 (2.8)	54 (0)	4 (0)	42 (0)	0 (0)	4
7 CH_3 deform. (A_1)	10.93 (3.0)	58 (0)	12 (0)	30 (0)	0 (0)	12
8 C−Br str. (A_1)	10.81 (6.4)	38 (4)	36 (0)	20 (4)	6 (2)	58

[a] A total of 100 trajectories were integrated for each initial condition with PES1(Br). The actual number of trajectories with the AM1-SRP surfaces is 50 but the listed numbers are scaled to 100 for comparison with PES1(Br). The maximum integration time for each trajectory is 25 ps. [b] Energies are in units of kcal/mol. Numbers in parentheses are the number of quanta added in the mode. In most cases, integral quanta were added so that the total internal energy (vibration + rotation), in excess of the Cl^- + CH_3Br classical asymptotic limit, is the Cl^-- - -CH_3Br harmonic zero-point energy plus approximately 2.7 kcal/mol. [c] The reactants are Cl^- + CH_3Br. [d] The products are $ClCH_3$ + Br^-. [e] A is the Cl^-- - -CH_3Br complex. [f] B is the $ClCH_3$- - -Br^- complex. [g] The number in parentheses is the number of trajectories of this type which have multiple crossings of the central barrier. A trajectory with an A → B crossing followed by a B → A crossing has multiple crossings.

calculations for Cl^-- - -CH_3Br → Cl^- + CH_3Br, is similar to that found previously[7] for Cl^-- - -CH_3Cl → Cl^- + CH_3Cl. The PES1(Br), AM1-SRP1, and AM1-SRP2 rate constants in Table 4 for Cl^-- - -CH_3Br and $ClCH_3$- - -Br^- dissociation agree to within a factor of 2. The Cl^-- - -CH_3Br → $ClCH_3$- - -Br^- isomerization rate constant is largest for the PES1(Br) surface, because the surface has the lowest isomerization barrier. The lower isomerization barrier and deeper $ClCH_3$- - -Br^- potential well, for the PES1(Br) surface as compared to the AM1-SRP surfaces, results in similar PES1(Br) and AM1-SRP RRKM rate constants for $ClCH_3$- - -Br^- → Cl^-- - -CH_3Br isomerization.

A previous study[7] has shown that anharmonicity lowers the rate constants for Cl^-- - -CH_3Cl dissociation and isomerization by approximately a factor of 2.[104] A similar anharmonic correction factor is expected for the Cl^-- - -CH_3Br complex. Thus, from the harmonic RRKM rate constants in Table 4 for the PES1(Br) and AM1-SRP surfaces, the anharmonic quantum RRKM lifetime of the Cl^-- - -CH_3Br complex is estimated to be in the range 4−6 ps. Therefore, quantum RRKM theory predicts nearly all of the Cl^-- - -CH_3Br complexes to decompose during the 25 ps the trajectories are integrated. Nearly all of this decomposition is to Cl^- + CH_3Br, with only 7.8, 0.9 and 1.8% crossing the central barrier to form $ClCH_3$- - -Br^- for the PES1(Br), AM1-SRP1, and AM1-SRP2 surfaces, respectively. The quantum harmonic RRKM lifetime for this latter complex is very short, i.e. 0.5−1.0 ps. Even though the isomerization barrier for Cl^-- - -CH_3Br has a lower potential energy than that for the dissociation channel (see Table 1), the RRKM rate constant for dissociation is much larger. This is because of the loose variational transition state for dissociation and the large rotational energy at the isomerization central barrier, due to the barrier's compact structure and resulting small moments of inertia.

As seen from Table 4, the anharmonic classical RRKM lifetimes for the Cl^-- - -CH_3Br complex are 4−6 times shorter than the analogous quantum values, for the PES1(Br) and AM1-SRP surfaces. Thus, both classical and quantum anharmonic RRKM theory predict that nearly all of the Cl^-- - -CH_3Br complexes should decompose on a 25 ps time scale. The percent of the Cl^-- - -CH_3Br complexes which isomerize to $ClCH_3$- - -Br^- is nearly the same for classical and quantum RRKM theory.

V. Direct Dynamics Trajectory Results

A. Comparison of the Results for the Different Potential Energy Surfaces. As shown in Table 5, similar numbers of the different types of events are observed for the PES1(Br) and AM1-SRP surfaces when the Cl^-- - -CH_3Br intermolecular modes are excited. When the A_1, C−Cl stretch is excited all of the complexes dissociate to Cl^- + CH_3Br for PES1(Br) and AM1-SRP2, while 96% form Cl^- + CH_3Br and 4% form $ClCH_3$ + Br^- for AM1-SRP1. Similar results are found for PES1(Br) and AM1-SRP1 when the E, Cl^- bend intermolecular mode is excited. Twelve percent of the trajectories form the $ClCH_3$ + Br^- products or remain in one of the complexes for both PES1-(Br) and AM1-SRP1. The number of these types of events is larger for AM1-SRP2.

In contrast, there are significant differences between the types of events for the PES1(Br) surface and the AM1-SRP surfaces, when the CH_3Br intramolecular modes are excited. Significantly less Cl^- + CH_3Br formation, more trajectories remaining in

(103) Hase, W. L.; Buckowski, D. G. *J. Comput. Chem.* **1982**, *3*, 335.

(104) The anharmonic correction was determined by convoluting an anharmonic density of states for the Cl^-- - -CH_3Cl intermolecular modes with a harmonic density of states for the CH_3Cl.

Table 6. Lifetimes of the Ion−Dipole Complexes of Quasiclassical Trajectories on the Different Potential Energy Surfaces[a]

		initial Cl^-- - -CH_3Br			Cl^-- - -CH_3Br after recrossing(s)		$ClCH_3$- - -Br^-	
excitation type	energy	diss.[b]		isom.[c]	diss.[d]	isom.[c]	diss.[e]	isom.[f]
				PES1(Br)				
1 Cl^- bend (E)	12.35 (60)	1.8		9.2		10.8	9.5	1.3
2 C−Cl str. (A_1)	12.48 (48)	0.005						
3 C−H str. (E)	12.52 (1.3)	15.5		8.5	3.4	0.6	6.8	2.2
4 C−H str. (A_1)	12.60 (1.4)	16.8		7.2	5.3	0.8	8.3	2.8
5 CH_3 rock (E)	12.45 (4)			8.4	4.2	0.5	8.0	2.3
6 CH_3 deform. (E)	12.45 (3)			6.8	2.7	0.4	8.1	2.2
7 CH_3 deform. (A_1)	12.58 (3)	11.9		7.2	7.5	0.6	8.1	2.2
8 C−Br str. (A_1)	12.86 (9)			0.2	0.2	0.8	9.6	2.4
				AM1-SRP1				
1 Cl^- bend (E)	12.44 (68)	5.9		15.0			8.0	
2 C−Cl str. (A_1)	12.35 (36)	6.7						
3 C−H str. (E)	12.37 (1.4)	10.4		4.3			15.8	
4 C−H str. (A_1)	12.42 (1.4)	8.7		6.9			4.5	
5 CH_3 rock (E)	12.01 (5)	10.5	10.3	8.6			8.8	
6 CH_3 deform. (E)	12.18 (3.2)	11.3	11.8					
7 CH_3 deform. (A_1)	12.43 (3.5)	10.9		9.7			5.5	
8 C−Br str. (A_1)	12.65 (7.5)	10.3	8.3	10.2	2.5		6.4	6.8
				AM1-SRP2				
1 Cl^- bend (E)	10.76 (44)	4.6	7.1	4.0				
2 C−Cl str. (A_1)	10.75 (34)							
3 C−H str. (E)	10.50 (1.2)	13.5	16.0	9.7			8.7	
4 C−H str. (A_1)	10.90 (1.2)	11.4	10.2					
5 CH_3 rock (E)	11.07 (4.4)	12.6	7.5					
6 CH_3 deform. (E)	10.74 (2.8)	13.1	21.9	2.6			3.4	
7 CH_3 deform. (A_1)	10.93 (3.0)	12.3	14.4	8.3			9.8	
8 C−Br str. (A_1)	10.81 (6.4)	11.1	8.4	3.0				3.4

[a] Lifetimes are in units of picosecond. [b] Dissociation to Cl^- + CH_3Br and direct dissociation to CH_3Cl + Br^-, respectively. [c] Isomerization to $ClCH_3$- - -Br^-. [d] Dissociation to Cl^- + CH_3Br. [e] Dissociation to $ClCH_3$ + Br^-. [f] Isomerization to Cl^-- - -CH_3Br.

the $ClCH_3$- - -Br^- complex, and more Cl^-- - -$CH_3Br \rightarrow ClCH_3$- - -$Br^-$ barrier crossings occur for PES1(Br) than for the AM1-SRP surfaces. Overall, more $ClCH_3 + Br^-$ products are formed with the analytic PES1(Br) surface than for the semiempirical AM1-SRP surfaces, but for several intramolecular mode excitations product formation is similar for the analytic and semiempirical surfaces. The percent of trajectories remaining in the Cl^-- - -CH_3Br complex is smallest for PES1(Br) and largest for AM1-SRP2.

Dissociation and isomerization average lifetimes for the Cl^-- - -CH_3Br and $ClCH_3$- - -Br^- complexes, calculated from the trajectories on the PES1(Br) and AM1-SRP surfaces, are listed in Table 6. Overall, the trajectory lifetimes for the different surfaces are in good agreement; i.e. they agree within a factor of 2.

B. Comparison with RRKM Theory. Before comparing the trajectory results with the RRKM predictions, it is useful to briefly review the results of the RRKM calculations in Section IV. The quantum anharmonic RRKM lifetime of the Cl^-- - -CH_3Br complex for the PES1(Br), AM1-SRP1, and AM1-SRP2 surfaces is estimated as 5, 6, and 4 ps, respectively. Thus, most of the complexes are predicted to have decomposed within the 25 ps time period investigated in the trajectories; i.e. for a lifetime of 5 ps, 99.3% are predicted to have decomposed. The classical anharmonic RRKM lifetime is shorter than the quantum value, so even more decomposition is predicted with the classical RRKM model. The classical model would be appropriate, if the classical motion is ergodic within the RRKM lifetime (assumption of RRKM theory) and, thus, the zero-point energy distributes freely between the vibrational modes.[103]

RRKM theory predicts most of the Cl^-- - -CH_3Br complexes to dissociate to Cl^- + CH_3Br instead of isomerizing to $ClCH_3$- - -Br^-. Different amounts of isomerization are predicted for the PES1(Br) and AM1-SRP surfaces, because of the different central barrier heights and Cl^-- - -CH_3Br well depths for the surfaces. The percent isomerization predicted by quantum RRKM theory for the PES1(Br), AM1-SRP1, and AM1-SRP2 surfaces is 7.8, 0.9, and 1.8, respectively, i.e. relative amounts of 8.7:1.0:2.0. Classical RRKM theory predicts only a slightly different percent isomerization, which is 8.5, 1.3, and 2.7 for the PES1(Br), AM1-SRP1, and AM1-SRP2 surfaces, respectively. With the RRKM predictions in hand, it is of interest to make comparisons with the trajectory results.

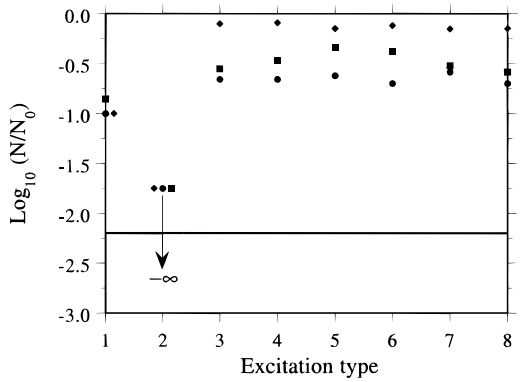

Figure 3. Logarithmic plot of the fraction of trajectories remaining undissociated on the 25 ps time scale for the different types of mode-specific excitations. The different excitation types are described in Tables 5 and 6 and in the text. The trajectory results are plotted for the PES1(Br) (◆), AM1-SRP1 (●), and AM1-SRP2 (■) surfaces. The solid line represents the prediction of RRKM theory for a complex lifetime of 5 ps.

The fraction of trajectories, remaining undissociated (i.e. either as Cl^-- - -CH_3Br or $ClCH_3$- - -Br^-) after 25 ps, is plotted in Figure 3 for the different types of mode-specific excitations. The RRKM prediction plotted in this figure is for a Cl^-- - -CH_3Br lifetime of 5 ps. The results for exciting either the Cl^-

Table 7. Cl^-- - -$CH_3Br \rightarrow ClCH_3 + Br^-$ Product Energy Partitioning[a]

	rel translation	rotation	vibration
AM1-SRP1	0.32	0.14	0.54
AM1-SRP2	0.24	0.09	0.67
PES1(Br)	0.09	0.06	0.85
experiment[b]	0.09		
OTS/PST[c]	0.18	0.26	0.56

[a] Numbers in the table are fractions of energy. [b] The experimental fraction of relative translational energy was calculated for 8 kcal/mol available energy in the reaction products. [c] The OTS/PST calculation is for an atom-sphere model for the products and is described in ref 6.

bend or C−Cl stretch intermolecular modes (excitation types 1 and 2) are similar for the PES1(Br) and AM1-SRP surfaces. All the complexes dissociate when the C−Cl stretch is excited, while less dissociation occurs than predicted by RRKM theory when the Cl^- bend is excited.

For each of the intramolecular mode excitations (excitation types 3−8), significantly less dissociation of the Cl^-- - -CH_3Br complex occurs than predicted by RRKM theory. The percentage of the trajectories which remain undissociated is 75, 22, and 34 for the PES1(Br), AM1-SRP1, and AM1-SRP2 surfaces, respectively. If an exponential dissociation probability is assumed (a very crude approximation), the respective dissociation lifetimes for the three surfaces are 87, 17, and 23 ps.

The percentage of the Cl^-- - -CH_3Br complexes which cross the central barrier in the trajectories to form either the $ClCH_3$- - -Br^- complex or the $Cl^- + CH_3Br$ product can also be compared with the RRKM prediction. As discussed above, the quantum RRKM value for this percentage is 7.8, 0.9, and 1.8 for surfaces PES1(Br), AM1-SRP1, and AM1-SRP2, respectively. The trajectory percentages, for the different excitation types, are found by adding the number of product and complex B events in Table 5. There is significant disagreement with RRKM theory with all the intramolecular mode excitations on the PES1(Br) surface and some of these excitations on the AM1-SRP surfaces. If the results of all the intramolecular mode excitations are combined for each surface, the percent isomerization is 86, 12, and 14 for surfaces PES1(Br), AM1-SRP1, and AM1-SRP2, and about ten times larger than the RRKM prediction for each surface. However, it is interesting that the relative amount of isomerization for the three surfaces follows the RRKM prediction. Nevertheless, both the dissociation and isomerization probabilities for the three surfaces disagree with the predictions of RRKM theory.

C. $ClCH_3 + Br^-$ Product Energies. The trajectories, which dissociated to the $ClCH_3 + Br^-$ products, were analyzed for product vibrational, rotational, and relative translational energies. By combining all the trajectories that formed the $ClCH_3 + Br^-$ products for a particular surface, average fractions of the available product energy released to vibration, rotation, and relative translation were determined. The $ClCH_3$ zero-point energy is excluded in calculating the vibrational energy. The results for the AM1-SRP1, AM1-SRP2, and PES1(Br) surfaces are listed in Table 7 where they are compared with the average fractions predicted by orbiting transition state/phase space theory (OTS/PST)[6] and the experimental value of Graul and Bowers[16,17] for the fraction released to translational energy. As discussed previously,[6] the trajectory results for PES1(Br) agree with the Graul and Bowers experiment. However, the AM1-SRP surfaces give relative translational energies which, on average, are approximately a factor of 3 too high. The fraction of energy released to vibration for the AM1-SRP surfaces is similar to the OTS/PST prediction.

VI. Conclusion

Direct dynamics simulations were performed of the unimolecular dynamics of the Cl^-- - -CH_3Br ion−molecule complex, which may be an important intermediate in the $Cl^- + CH_3Br \rightarrow ClCH_3 + Br^-$ S_N2 nucleophilic substitution reaction. Two different potential energy surfaces, identified as AM1-SRP1 and AM1-SRP2, were investigated in the simulations by using the AM1 semiempirical model, with two different sets of specific reaction parameters (SRPs). Each direct dynamics trajectory was integrated for 25 ps or until either $Cl^- + CH_3Br$ or $ClCH_3 + Br^-$ was formed. The results of the simulations on the two AM1-SRP surfaces were compared with those determined previously from simulations on the PES1(Br) analytic potential energy function, which was developed by fitting *ab initio* calculations and experimental energies, geometries, and frequencies. The AM1-SRP1, AM1-SRP2, and PES1(Br) surfaces are qualitatively the same, but they have quantitative differences in stationary point properties, such as geometries and frequencies, the Cl^-- - -CH_3Br well depth, and the $[Cl$- - -CH_3- - -$Br]^-$ central barrier height. For the total energy and angular momentum considered in the simulations, the relative RRKM rate constants for Cl^-- - -$CH_3Br \rightarrow Cl^- + CH_3Br$ dissociation on the AM1-SRP1, AM1-SRP2, and PES1(Br) surfaces are 0.61:1.00:0.65, while the relative Cl^-- - -$CH_3Br \rightarrow ClCH_3$- - -$Br^-$ isomerization RRKM rate constants are 0.10:0.33:1.00.

The simulations, for each of the three surfaces, show that the probability the trajectories remain undissociated (i.e., either as Cl^-- - -CH_3Br or $ClCH_3$- - -Br^-) depends on the type of mode initially excited in the Cl^-- - -CH_3Br complex. Exciting the Cl^-- - -C intermolecular stretch mode leads to rapid dissociation, much faster than the RRKM prediction, to preferentially form $Cl^- + CH_3Br$. When the CH_3Br intramolecular modes of the complex are excited, the fraction of trajectories which remain undissociated is much larger than predicted by RRKM theory. The dissociation rate is closest to the RRKM prediction when the Cl^- bend intermolecular mode is excited.

Exciting the CH_3Br intramolecular modes of the Cl^-- - -CH_3-Br complex enhances Cl^-- - -$CH_3Br \rightarrow ClCH_3$- - -$Br^-$ isomerization for each of the three surfaces. For PES1(Br) the probability of isomerization is relatively insensitive to which intramolecular mode is excited, while for the two AM1-SRP surfaces isomerization becomes particularly efficient when the C−Br stretch intramolecular mode is excited. If the results of all the intramolecular mode excitations for each surface are combined, the fraction of the trajectories, which cross the central barrier to isomerize to $ClCH_3$- - -Br^- or form $ClCH_3 + Br^-$ instead of dissociating to $Cl^- + CH_3Br$, is found to be approximately a factor of 10 higher than the RRKM prediction for each surface. Thus, with the intramolecular mode excitations, the relative amounts of isomerization for the three surfaces agree with RRKM theory, while the absolute amounts do not.

Though the mode-specific dissociation and isomerization probabilities for the three surfaces show similar disagreement with the predictions of RRKM theory, there are important differences in the detailed dynamics of the three surfaces when the intramolecular modes are excited. There is significantly less $Cl^- + CH_3Br$ formation, more $ClCH_3 + Br^-$ formation, and more trajectories remaining in the $ClCH_3$- - -Br^- complex for PES1(Br) than for the two AM1-SRP surfaces. The probability of remaining in the Cl^-- - -CH_3Br complex is smallest for PES1(Br) and largest for AM1-SRP2. If the intramolecular and unimolecular dynamics of the Cl^-- - -CH_3-Br and $ClCH_3$- - -Br^- were statistical, such differences would not be expected. Instead, detailed aspects of the nonstatistical

dynamics observed in the trajectories depend on specific features of the potential energy surfaces.

Of the three surfaces investigated for Cl^-- - -CH_3Br dissociation, only PES1(Br) gives $ClCH_3 + Br^-$ product energy partitioning in agreement with the experiments of Graul and Bowers.[16,17] The AM1-SRP surfaces give an average product relative translational energy approximately a factor of 3 too large.

In conclusion, two points should be emphasized. First, the type of nonstatistical dynamics observed in the simulations of Cl^-- - -CH_3Br decomposition are for small total angular momentum and may only indirectly pertain to the $Cl^- + CH_3Br \rightarrow ClCH_3 + Br^-$ reaction, which is dominated by collisions with large total angular momentum. Second, different potential energy surfaces for a unimolecular reactive system may be derived so that they have the same stationary point properties (i.e., energies, geometries, and vibrational frequencies) and, possibly, even similar reaction path properties, so that they give the same RRKM rate constants. However, if the reaction dynamics is nonstatistical, dynamical calculations performed on the different surfaces will not yield the same attributes such as rate constants, branching ratios, product energies, etc. unless global properties of the surfaces are the same. The simulations reported here indicate this is the situation for the $Cl^- + CH_3Br \rightarrow ClCH_3 + Br^-$ reactive system. Additional support for this proposition comes from reduced dimensionality quantum dynamical calculations of the rate constant for $Cl^- + CH_3Br$ nucleophilic substitution using PES1(Br).[105] Making only minor changes in the central barrier geometry, while retaining the PES1(Br) barrier height and vibrational frequencies, alters the reaction mechanism from one where extensive trapping in the Cl^-- - -CH_3Br and $ClCH_3$- - -Br^- complexes occurs to one involving direct substitution without trapping in the complexes. The implication is that a quantitative calculation of all the dynamical attributes of the $Cl^- + CH_3Br \leftrightarrow Cl^-$- - -$CH_3Br \leftrightarrow ClCH_3$- - -$Br^- \rightarrow ClCH_3 + Br^-$ reactive system may require the use of a potential energy surface derived from high-level *ab initio* calculations.

Acknowledgment. Preliminary reports of this research have been given at the International Symposium on Computational Molecular Dynamics, University of Minnesota Supercomputer Institute, Minneapolis, MN, October 24−26, 1994, and at the 10th University of Waterloo Symposium on Chemical Physics, November 1994, Waterloo, Canada. This research was supported by the National Science Foundation. The authors wish to acknowledge helpful conversations with Peter Botschwina, David Clary, Evi Goldfield, Berny Schlegel, and Sigrun Seeger. This paper was written while Bill Hase visited the Reinhard Schinke research group at the Max-Planck-Institut für Strömungsforschung in Göttingen, Germany.

JA953120T

(105) Clary, D. C. Private communication.